Electrical Transport in Polymer-Covered Silicon Nanowires

K. Fobelets, *Senior Member, IEEE*, P. Ding, N. Mohseni Kiasari, and Z. Durrani

***Abstract*—The influence of polymer layers wrapped around n-type Si nanowires (NW) on their electrical characteristics is investigated. The NWs are fabricated via metal induced excessive oxidation and dissolution of Si, and have a diameter of ∼350 nm. Single wires are covered by various polymer layers. The polymers used are both insulating [poly (methyl methacrylate) (PMMA), polyethylene (PE), polystyrene, and polyethylene oxide (PEO)] and semiconducting poly (3,4-ethylenedioxythiophene):poly (styrenesulfonate). Four-point probe measurements are used to measure the conductivity changes of single NWs. The NW resistivity increases with PE and PMMA coverage, but decreases with PEO coverage. The changes are attributed to carrier exchange between the polymer and NW. The measurements also confirm active electron trapping with PE coverage that is not observed with the other polymers.**

***Index Terms*—Composite, nanowires (NWs), polymer, surface treatment.**

I. Introduction

In RECENT years, there has been great interest in Si nanowires (NWs) as a consequence of their potential importance for sensors, and for optical and electronic applications [1]. Two key issues in the application of Si NWs are: the control of their thermal and electrical conductivity and their (self-) assembly into certain positions within circuits. It is well known that the large surface to volume ratio in NWs results in electrical transport highly sensitive to the surface condition of the wire [2]. This suggests that the NWs' electrical conductivity can be tailored using surface-modification techniques. In bulk Si, the electrical conductivity is varied via dopant implantation. However, for doping densities larger than $\sim 10^{16}$ cm^{-3}, impurity scattering decreases the mobility and thus the conductivity [3]. In principle, dopant implantation can also be used to change the conductivity in NWs. Though, damage to the NW structure during implantation, and for NWs with diameter ∼10 nm, the statistical character of the position of the doping atoms can create local electrostatic potential variations and lead to mobility degradation [4].

Manuscript received December 14, 2009; revised February 12, 2010; accepted April 4, 2010. Date of publication May 6, 2010; date of current version July 11, 2012. This work was supported by the Engineering and Physical Sciences Research Council (EPSRC), under Grant EP/F027753/1. The review of this paper was arranged by Associate Editor A. A. Balandin.

The authors are with the Electrical and Electronic Engineering Department, Imperial College London, SW7 2AZ, South Kensington, U.K. (e-mail: k.fobelets@imperial.ac.uk; peiwding@googlemail.com; mohseni.nima@gmail.com; z.durrani@imperial.ac.uk).

Color versions of one or more of the figures in this paper are available online at http://ieeexplore.ieee.org.

Digital Object Identifier 10.1109/TNANO.2010.2049746

TABLE I
Electronic Properties of the Materials From Various Sources

Property / Material	Work function (eV)	Electron affinity (eV)	Ionization energy IE (eV)
Lowly-doped n-Si	4.3 [3]	4.05 [3]	5.15 [3]
PE	4.9 [11]	-0.14 [12]	8.8 [12]
PS	4.9 [11]	0.4 [13]	6.95 [13]
PMMA	4.68 [11]	0.65 [14]	9.21 [14]
PEO	3.95 [11]		
PEDOT:PSS	4.7–5.1 [15]	2.2 [16]	5 [17]

The easy adsorption of molecules on the surface of the NWs can influence the conductivity in an uncontrolled manner. Different methods exist to manage the condition of the surface of NWs. While traditional surface passivation techniques such as the thermal growth of SiO_2 protect the NW and reduce surface defects, they may also greatly influence carrier concentrations and mobilities [5], [6]. Hydrogen treatment is used both in bulk Si, as well as in Si NWs, to neutralize defects on the surface of the Si [7]. Chemical treatment of the Si NW surfaces with organic compounds may also be used for trap reduction and surface passivation [8]. The use of coatings as, e.g., diamond has also been reported to dramatically improve thermal and electrical properties of Si NWs [9], [10]. Control of the trap density at the surface of the wires is essential for maintaining the electrical performance of NWs, and for minimizing aging effects due to surface reactions.

In this study, we investigate how covering Si NWs in polymers changes their conductivity, and how this conductivity change is dependent on the doping type. Experiments were carried out on low-doped n-type Si NWs and low-doped p-type thin Si SOI films (doping level: $\sim 10^{16}$ cm^{-3}). We encapsulate the Si NWs with polymers dissolved in solvents and spun in liquid form onto the wire. We use the following polymers: Poly (methyl methacrylate) (PMMA), Polyethylene (PE), Polystyrene (PS), Polyethylene oxide (PEO), and poly (3,4-ethylenedioxythiophene):poly (styrenesulfonate) (PEDOT:PSS). PE, PS, PEO and PMMA are insulating polymers and PEDOT:PSS is a semiconductor. Table I summarizes the electronic properties of all materials used [11]–[17].

Note that the insulating polymers have a very low electron affinity, in general, one order of magnitude smaller than the value for Si. This would imply, if dipole moments are ignored, that for all the polymers, the highest occupied molecular orbital/lowest unoccupied molecular orbital (LUMO/HOMO) levels are offset from the conductance/valence band in Si. In order to make a simple prediction of the influence of the polymer, one

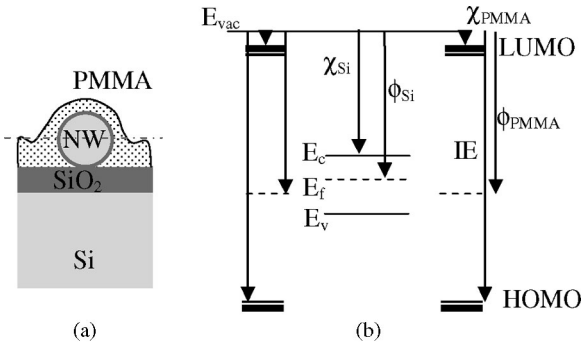

Fig. 1. (a) Schematic cross section of a polymer-wrapped NW on SiO_2. (b) Energy bands through the cross section of the wire along the dashed line in (a) before contact. The energy band of the thin native oxide layer is not drawn. E_c, E_v, and E_f are, respectively, the bottom of the conduction band, the top of the valence band, and the Fermi level.

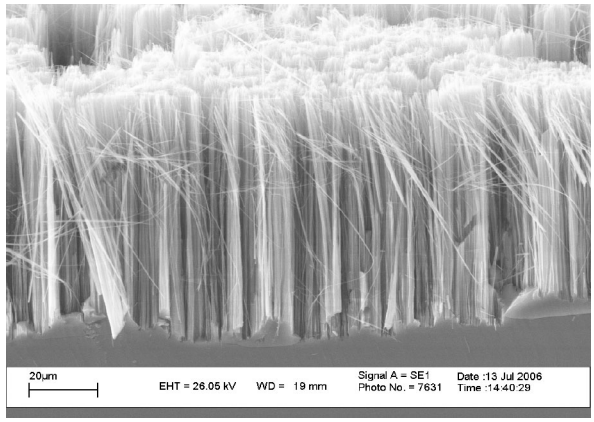

Fig. 2. SEM Cross section of an array of Si NWs made by metal-induced excessive local oxidation and dissolution of a Si wafer and after removal of the Ag layer.

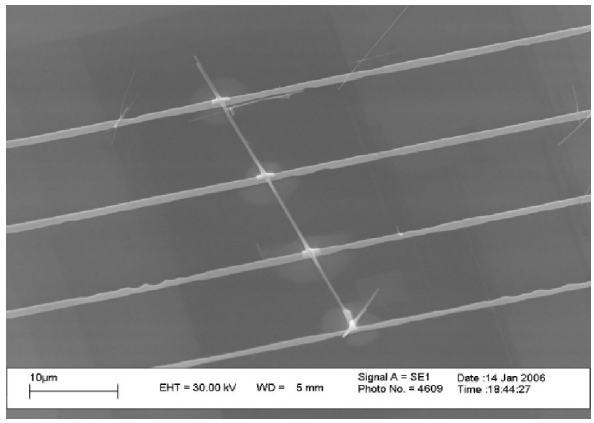

Fig. 3. SEM picture of a Si NW on the four Au lines of the four-point probe structure on SiO_2. At each crossing between Au and Si NW, a thin, small layer of Pt is deposited by FIB to reinforce the contacts and improve the ohmic behavior.

can, for a first approximation, use the work function difference between the polymer and Si. However, dipoles may exist in the polymer, caused by interface states or the possible polar character of the polymer. These dipoles can influence the position of the LUMO/HOMO levels in the polymer relative to the conduction/valence band in the Si NW [18]. The work function difference may also cause electron depletion/accumulation at the surface of the low n-doped Si NWs after polymer coverage. A schematic energy band alignment is given in Fig. 1.

PS and PMMA both are believed to reduce the concentration of interfacial traps [19], [20] and are, therefore, ideal for protection of the surface of the NWs. PE and PS are nonpolar, although the individual molecules can have a large dipole moment [21]. PMMA, PEO, and PEDOT:PSS, however, are polar with various magnitudes of dipole moment [21]. The existence of the surface dipole will change the band bending imposed by the electron-affinity rule and thus have an influence on the magnitude of the change of the conductivity of the NW when wrapped in the polymer.

II. Material Preparation

The Si NWs are fabricated using metal-induced excessive local oxidation and dissolution of a Si wafer using electroless plating in $HF/AgNO_3$, followed by an etch in an aqueous $HF/Fe(NO_3)_3$ solution [22]. The process forms NWs with a diameter between 100 and 400 nm and a uniform length up to $\sim$300 μm. The average wire diameter depends on the doping of the Si wafers used as start material, with heavy p-type doped wafers giving thinner wires. Doping concentration may also affect the crystallinity of the NWs [23]. The low doping level chosen for our wires results in crystalline material.

Fig. 2 gives the SEM image of an array of NWs obtained after etching. The NWs are harvested via ultrasonic agitation in isopropyl alcohol and are then dispersed on a preprocessed SiO_2-on-Si wafer. The SiO_2 layer is 1 μm thick and thermally grown. The NW concentration in solution is kept low for control of the density of the dispersed wires. The wafer also contains a suitable geometry for four-point probe measurements [24]. This consists of four equidistant Au lines (2 μm in width), leading to large contact regions (each 100×100 μm^2) for electrical probe measurements. Four-point probe measurements are essential for the extraction of the resistivity of the Si NW without the influence of the contact resistances. An SEM picture of a Si NW lying across the four Au contact lines of the four-point probe geometry is given in Fig. 3. In these measurements, a current is driven through the outer contacts and the voltage drop between the inner two contacts is measured with a high-impedance voltmeter. In our initial four-point probe structures, it was found that the Au contacts to the NW were rectifying in both bias directions and that, due to the simple NW dispersion technique on the preprocessed sample, multiple wires could potentially contact two or more of the Au lines. We used focused ion beam (FIB) to first deposit Pt locally on the crossing points between the NW and the Au lines, and second to ion-mill all other wires that could potentially short the Au contact lines. The contacts were then annealed for 90 s in an Ar ambient at 500 °C in an rapid thermal annealing. This annealing resulted in good ohmic contacts.

Although the contact resistance should not be important in a four-point probe measurement, the annealing of the contacts

avoids current rectification and improves the accuracy of measurements at low current levels. As a result of annealing, the currents are higher and the voltage difference generated between the contacts remains within acceptable values (<20 V). At larger current levels and thus higher potential differences across the Si NW, self-heating effects can influence the resistance measurements of the wires. These self-heating effects can be expected as the Si NWs are lying on SiO_2 and are covered in a native oxide layer [25]. Coverage of the wire in polymers aggravates the self-heating. As a consequence, good ohmic contacts are essential for accurate resistance extraction at low current levels.

The diameter of the n-Si NW used in these measurements is ~350 nm. Four different polymers were spin-coated across the Si NW assembled on a four-point probe structure. Since the NW touches the SiO_2 substrate layer, the polymer does not cover the NW completely. The PMMA film was formed from a solution of 5 wt% PMMA in toluene, the PE and PS film from a solution of 5%wt PE in decalin, and the PEO film from a solution of 5 wt% PEO in H_2 O. All polymer films were found to be insulating. The conductivity of the chemically prepared and spin-coated PEDOT:PSS is relatively low ($\sigma \approx 0.03\ (\Omega{\cdot}\mathrm{cm})^{-1}$) and is at least ten times smaller than the Si substrate from which the NW have been fabricated [26]. PEDOT:PSS is typically used as a p-type semiconducting polymer in organic LEDs. Before measurements, the polymer is removed from the outer contacts of the four-point probe structure by scratching the surface with a probe needle such that direct contact to the Au probing pad can be made.

III. Results and Discussion

The resistance of the Si NW was measured before and after polymer deposition, over a current range between -5×10^{-4} and 5×10^{-4} A. The ratio of the measured voltage across the inner four-point probe contacts to the current through the outer four-point probe contacts was plotted as a function of current. Near constant resistance as a function of drive current was calculated from the measurements. A slight decrease of 10% was seen in current for the highest drive current ($\pm 5 \times 10^{-4}$ A) for both the covered and bare Si NW. This decrease in current is probably due to self-heating effects in the Si NW, which increases the carrier concentration. The measurement was repeated four times on the same NW in order to obtain an average. An example of a measurement using PMMA is given in Fig. 4.

In Fig. 5, all results of the four-point probe measurements are given at 10^{-4} A only. Note that for the PEO experiment, a second n-Si NW etched from a Si wafer with higher resistivity was used. There is, therefore, another "bare NW" measurement for comparison with the PEO measurement (see second wire in Fig. 5). The resistivity measurements were repeated on p-type material. In order to reduce the complexity of the preparation, van der Pauw measurements were carried out on thin p-Si body silicon-on-insulator (SOI) material [24]. This gives a good qualitative approximation to the NW coverage, sufficient to compare n-type versus p-type Si behavior and support the work function-related carrier transfer picture. For the van der Pauw measurements, mesas were etched in the thin p-Si body down to the buried oxide layer. Here, the Si body was 150 nm thick, while the buried oxide layer was 100 nm thick. The same insulating polymers, including PS were dissolved and spun onto the mesa. Van der Pauw measurements were done on a large number of mesas (>10) in order to obtain an average resistance change. The current densities used in these measurements were lower than those used for the n-Si, as oxide breakdown can occur at lower voltage differences across the thin buried oxide layer. The results of these measurements are also given in Fig. 5.

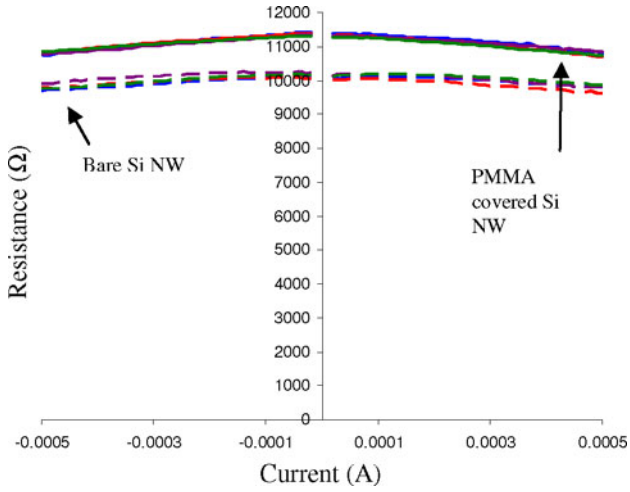

Fig. 4. Resistance across the inner contacts of the four-point probe setup as a function of the current through the outer contacts. Dashed line: bare Si NW; full line: PMMA-covered Si NW.

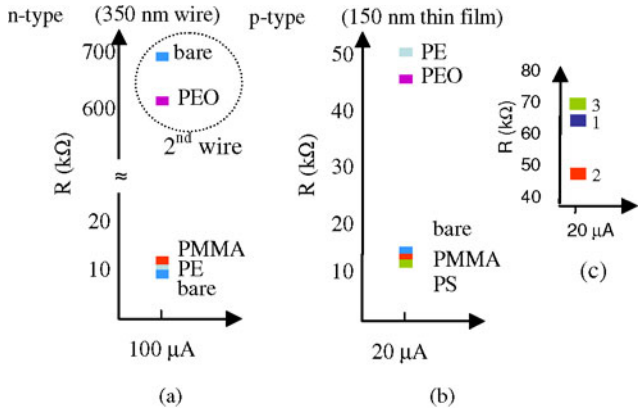

Fig. 5. (a) Resistance of the polymer covered n-type Si NW compared to the bare Si NW. The measurements for PEO were done on high-resistivity Si NWs (second wire). (b) Resistance of the polymer-covered p-type Si thin film relative to the bare thin film. (c) influence of e-beam radiation of PE. 1—PE-covered p-Si, 2—freshly irradiated PE, and 3—five days after irradiation.

Table II summarises the resistivity change. The resistivity is estimated from the classical formulae for thin films [24]

$$\rho = \frac{\pi t}{\ln(2)} \left(\frac{V}{I} \right)$$

where t is the diameter/thickness of the wire/film.

Comparing the resistivity changes on n-Si to those on p-Si show opposite resistance changes for the same polymer coverage, except for PE. Unlike the other polymers used, PE contains active electron traps [27], [28]. In order to investigate this

TABLE II
PERCENTAGE CHANGE IN RESISTIVITY OF THE SI NW AFTER COVERAGE BY DIFFERENT POLYMERS

polymer	ϕ (eV)	$\Delta\rho$ % (n-Si (350 nm))	$\Delta\rho$ % (p-Si (150 nm))
PS	4.9	NA	-12
PE	4.9	8	380
PMMA	4.68	13	-7
PEO	3.95	-13	280

Work function ϕ for all polymers is also given. Negative signs mean decrease in resistivity with polymer coverage.

further, a PE-covered p-Si thin film was measured and then irradiated with an electron beam in the SEM ($I_{\mathrm{beam}} = 300\,\mathrm{pA}$, EHT $= 20\,\mathrm{kV}$, causing small electron penetration depths into the polymer). After e-beam irradiation, the PE-covered p-Si thin film was measured immediately, and then remeasured after 5 days in ambient. We notice that the resistance of the wire decreases after e-beam irradiation and that the original resistance value is restored after aging of the film. This is consistent with the existence of electron traps in the PE layer. Unfilled trapping centers are positively charged and cause depletion of mobile holes at the surface of the p-Si layer. Irradiation with electrons neutralizes the traps in PE, caused by surface charging and/or electron penetration, such that more carriers remain in the p-Si and a lower resistance is measured. Over time, the electrons are released from the traps, restoring the resistance increase. For the n-Si NWs, the electrons that fill the PE trap centers are supplied by the NW, causing an increase in resistance.

To first approximation, the results of the four-point probe measurements, except for PE, seem to suggest that the resistivity changes are consistent with the work function difference between Si and polymer. However, the amplitude of the resistivity variation is not consistent with the difference in work function. This can be caused by differences in work function of our polymers to the values in the literature, by the effect of the remaining nonneutralized traps at the insulator/semiconductor interface, or by the polarity of (broken) polymer chains.

The variation of the current through the n-Si NW after coverage with PEDOT:PSS is given in Fig. 6. Fig. 6 shows the current–voltage characteristics of the bare NW, the NW freshly covered with PEDOT:PSS, and the latter system measured after four days. The bare Si NW shows near ohmic behavior due to good FIB reinforced Pt contacts. In the Si NW, freshly covered with PEDOT:PSS, the conductivity increases in a nonlinear manner, with an increase in the conductivity at higher voltages. This increase can be associated with changes in the polymer at higher voltages. Furthermore, due to the work function difference between polymer and n-Si, band bending at the polymer/semiconductor interface causes depletion in the n-Si layer. This results in a lower total current (see negative bias) even at low voltage, notwithstanding any parallel conduction via the polymer. At higher voltages, $PEDOT^{+}$ and PSS^{-} segregate, causing a change in band bending at the Si surface and eliminating the depletion region created by the work function difference. In addition, the PEDOT:PSS layer goes into a low-conductivity state, reducing the parallel conductance [29]. After aging, a current offset occurs, which may be due to charge detrapping in the polymer layer, or due to the dipole moment introduced by the polymer. The shape of the curve in the high-voltage region also changes due to the increased resistivity of the PEDOT:PSS layer after aging. The aging effect needs to be further investigated, but is possibly due to ion-exchange processes between the polymer film and Si in air [26].

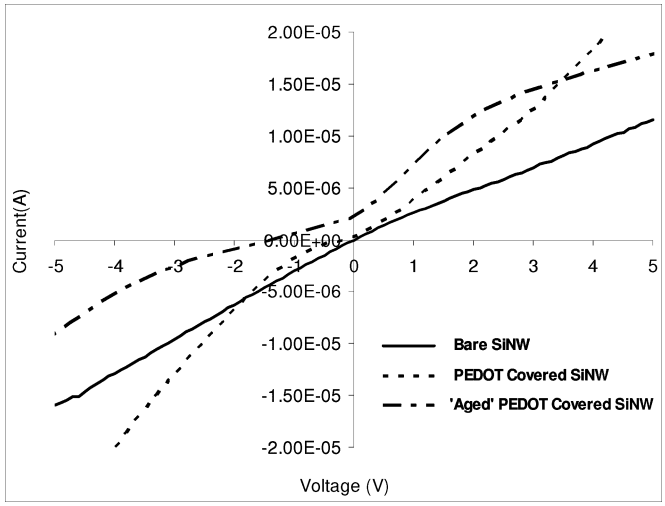

Fig. 6. Current–voltage characteristic of a fresh and "aged" PEDOT:PSS-covered Si NW compared to the uncovered Si NW.

IV. CONCLUSION

The conduction of Si NWs covered by various polymer layers is investigated. To a first approximation, the qualitative changes in resistivity of the Si NWs are consistent with the work function difference between the wires and the polymer wrapping. However, the quantitative analysis is strongly dependent on charged states in the polymer layer and possible dipole moments. Clear electron-trapping effects were observed for NWs covered with PE. Covering of Si NWs with the semiconducting polymer PEDOT:PSS leads to nonlinear current increase at higher applied voltages and current/voltage offsets after aging.

ACKNOWLEDGMENT

The authors would like to thank V. Stevens for fabrication of the wires and M. Ahmad and M. Green for useful discussions.

Focused ion beam was carried out under the EPSRC-funded Equipment Access Scheme in the Center for Nanotechnology, London, U.K.

REFERENCES

[1] M. Law, J. Goldberger, and P. Yang, "Semiconductor nanowires and nanotubes," *Ann. Rev. Mat. Res.*, vol. 34, pp. 83–122, 2004.
[2] Y. Cui, Z. Zhong, D. Wang, W. U. Wang, and C. M. Lieber, "High performance silicon nanowire field effect transistors," *Nano Lett.*, vol. 3, pp. 149–152, 2003.
[3] S. M. Sze, *Physics of Semiconductor Devices*. New York: Wiley, 1981.
[4] A. Asenov, "Random dopant induced threshold voltage lowering and fluctuations in sub-0.1 μm MOSFET's: A 3-D "atomistic" simulation study," *IEEE Trans. Electron. Dev.*, vol. 45, pp. 2505–2513, 1998.

[5] J. Jie, W. Zhang, K. Peng, G. Yuan, C. S. Lee, and S. T. Lee, "Surface-dominated transport properties of silicon nanowires," *Adv. Funct. Mater.*, vol. 18, pp. 3251–3257, 2008.

[6] K. Seo, S. Sharma, A. A. Yasseri, D. R. Stewart, and T. I. Kamins, "Surface dharge density of unpassivated and passivated metal-catalyzed silicon nanowires," *Electrochem. Solid-State Lett.*, vol. 9, pp. G69–G72, 2006.

[7] N. Fukata, J. Chen, T. Sekiguchi, S. Matsushita, T. Oshima, N. Uchida, K. Murakami, T. Tsurui, and S. Ito, "Phosphorus doping and hydrogen passivation of donors and defects in silicon nanowires synthesized by laser ablation," *Appl. Phys. Lett.*, vol. 90, pp. 153117–3, 2007.

[8] M. Nolan, S. O'Callaghan, G. Fagas, and J. C. Greer, "Silicon nanowire band gap modification," *Nano Lett.*, vol. 7, pp. 34–38, 2007.

[9] V. A. Fonoberov and A. A. Balandin, "Giant enhancement of the carrier mobility in silicon nanowires with diamond coating," *Nano Lett.*, vol. 6, pp. 2442–2446, 2006.

[10] E. P. Pokatilov, D. L. Nika, and A. A. Balandin, "Acoustic phonon engineering in coated cylindrical nanowires," *J. Superlattices and Microstructures*, vol. 38, pp. 168–183, 2005.

[11] C. F. Gallo and W. L. Lama, "Classical electrostatic description of the work function and ionization energy of insulators," *IEEE Trans. Indust. Appl.*, vol. IA-12, pp. 7–11, 1976.

[12] M.C. Righi, S. Scandolo, S. Serra, S. Iarlori, E. Tosatti, and G. Santoro, "Surface states and negative electron affinity in polyethylene," *Phys. Rev. Lett.*, vol. 87, pp. 76802–4, 2001.

[13] N. Ueno, K. Sugita, K. Seki, and H. Inokuchi, "Electron affinities of polystyrene and poly(2-vinylpyridine) by low-energy electron inelastic scattering," *Jpn. J. Appl. Phys.*, vol. 24, pp. 1156–1163, 1985.

[14] S. M. Sayyah, A. B. Khaliel, and H. Moustafa, "Electronic structure and ground state properties of PMMA polymer: I. Step-by-step formation and stereo-regularity of the polymeric chain—AM1-MO treatment," *Int. J. Polymeric Mat.*, vol. 54, pp. 505–518, 2005.

[15] T. M. Brown, J. S. Kim, R. H. Friend, F. Caciallia, R. Daik, and W. J. Feast, "Built-in field electroabsorption spectroscopy of polymer light-emitting diodes incorporating a doped poly(3,4-ethylene dioxythiophene) hole injection layer," *Appl. Phys. Lett.*, vol. 75, pp. 1748–1751, 1999.

[16] T. Zhang, Z. Xu, D. L. Tao, F. Teng, F. S. Li, M. J. Zheng, and X. R. Xu, "The influence of ZnO nanorods on the poly-(3,4-ethylenedioxythiophene):poly-(styrenesulphonic acid) buffer layer in a polymer light-emitting diode," *Nanotechnology*, vol. 16, pp. 2861–2865, 2005.

[17] S. Nishino, J. Okada, K. Kumazawa, and T. Mori, "Modification of ionization potential of poly(ethylene dioxythiophene):poly(styrene sulfonate) film by acid or base treatment," *Jpn. J. Appl. Phys.*, vol. 46, pp. 7427–7431, 2007.

[18] D. Cahen and A. Kahn, "Electron energetics at surfaces and interfaces: concepts and experiments," *Adv. Mater*, vol. 15, pp. 271–277, 2003.

[19] T. Takahashi, T. Takenobu, J. Takeya, and Y. Iwasa, "Ambipolar light-emitting transistors of a tetracene single crystal," *Adv. Funct. Mat.*, vol. 17, pp. 1623–1628, 2007.

[20] B. Park, I. In, P. Gopalan, P. G. Evans, S. King, and P. F. Lyman, "Enhanced hole mobility in ambipolar rubrene thin film transistors on polystyrene," *Appl. Phys. Lett.*, vol. 92, pp. 133302–3, 2008.

[21] D.I. Bower, *An introduction to polymer physics*. Cambridge, U.K.: Cambridge Univ. Press, 2004.

[22] K. Q. Peng, J. J. Hu, Y. J. Yan, Y. Wu, H. Fang, Y. Xu, S.T. Lee, and J. Zhu, "Fabrication of single-crystalline silicon nanowires by scratching a silicon surface with catalytic metal particles," *Adv. Funct. Mater.*, vol. 16, pp. 387–394, 2006.

[23] A. I. Hochbaum, D. Gargas, Y. J. Hwang, and P. Yang, "Single crystalline mesoporous silicon nanowires," *Nano Lett*, vol. 9, pp. 3550–3554, 2009.

[24] D. K. Schröder, *Semiconductor material and device characterization*. New York: Wiley, 1998.

[25] B. M. Tenbroek, M. S. L. Lee, W. Redman-White, J. T. Bunyan, and M.J. Uren, "Self-heating effects in SOI MOSFETs and their measurement by small signal conductance techniques," *IEEE Trans. Electron Dev.*, vol. 43, pp. 2240–2248, 1996.

[26] X. Crispin, S. Marciniak, W. Osikowicz, G. Zotti, A. W. Denier Van DerGon, F. Louwet, M. Fahlman, L. Groenendaal, F. De Schryver, and W. R. Salaneck, "Conductivity, morphology, interfacial chemistry, and stability of poly(3,4-ethylene dioxythiophene)–poly(styrene sulfonate): A photoelectron spectroscopy study," *J. of Polymer Science B: Polymer Physics*, vol. 41, pp. 2561–2583, 2003.

[27] R. H. Partridge, "Electron traps in polyethylene," *J. Polymer Sci. A*, vol. 3, pp. 2817–2825, 1965.

[28] C. Perrin, V. Griseri, C. Inguimbert, and C. Laurent, "Analysis of internal charge distribution in electron irradiated polyethylene and polyimide films using a new experimental method," *J. Phys. D: Appl. Phys.*, vol. 41, pp. 205417–4, 2008.

[29] X. Xu, R. A. Register, and S. R. Forrest, "Mechanisms for current-induced conductivity changes in a conducting polymer," *Appl. Phys. Lett.*, vol. 89, pp. 142109–3, 2006.

Authors' biographies and photographs not available at the time of publication.